Advanced in Computer-Aided Bearing Design
Edited by: Chang, C.M. and Kennedy, F.E.,
ASME-ASLE Lubrication Conference,
October 5-7, 1987, Washington DC
American Society of Mechanical Engineers
(ASME) Publication G-00220

SIMULATION OF LOW FREQUENCY COMPONENTS IN THE DYNAMIC RESPONSE OF A BALL BEARING

P. K. Gupta
Mechanical Technology Incorporated
Latham, New York

ABSTRACT

Suitable equilibrium constraints are introduced in the existing computer code DREB to greatly increase the permissible time step size and thereby provide bearing performance simulation over large time intervals within acceptable computational effort. The modified code, RAPIDREB, has proven to be very efficient in simulating ball bearing performance over several shaft revolutions. Hence, simulation of the very low frequency components has been possible. The code RAPIDREB is applied to a typical turbine engine ball bearing to examine cage whirl and subsequent failure due to excessive wear of the cage surface interacting with the guiding raceway.

INTRODUCTION

Computer simulation of the performance of rolling bearings has proven to be a very effective means of designing some of the most advanced rolling bearing systems. The available computer codes provide both a simple static equilibrium solution and a full transient simulation obtained by integration of the differential equations of motion of the various bearing elements. As reviewed by Gupta (1) and Sibley and Pirvics (2), there have been a large number of programs aimed at solving the static equilibrium problem with varying levels of sophistication. Dynamic simulation codes, however, have been rather few; the most noted works have been due to Walters (3), Gupta (4-7) and more recently due to Brown et al (8). Since the dynamic codes perform a real time integration of a large number of differential equations of motion, the computational effort required by any of the dynamic computer programs has been a practical limitation. This is related directly to the nature of the model in the sense that the maximum step size for the numerical integration of a system of differential equations of motion is determined by the highest frequency present in the system, which is often several orders of magnitude higher than the shaft rotational speed. In order to simulate effects of the order of shaft speed, integration over a very large time domain is required and since the maximum step size is limited by the high frequencies, the computing costs, especially for very low speed applications, have proven to be prohibitive. The primary objective of the present investigation is to review the various time scales in the general behavior of a ball bearing and by selectively suppressing the very high frequencies, develop a "rapid version" of the DREB (Dynamics of Rolling Element Bearings) computer program developed earlier

by the author (4-7). This new version of the program has been designated as RAPIDREB.

For a typical ball bearing the high frequency present in the system is defined by the ball/race Hertzian contact. If the ball is free to translate, vibratory motion corresponding to this natural frequency has been observed. Also, a relatively high frequency is also associated with the kinematics of ball motion (9). In order to suppress these high frequencies the ball mass center may be constrained in a suitable manner. Once this is done the step size can be made relatively large and integration over a prescribed time domain can be carried out much more effectively.

This paper considers an equilibrium constraint, where the position of ball mass center at any instant is determined by satisfying the radial and axial equilibrium of forces on the ball. Thus the ball now moves freely in a four-degrees-of-freedom system, i.e., orbital motion of ball mass center, and the three rotations about the mass center. The constraint is very similar to the one used by Walters (3) except that the equilibrium is performed at each time step and the generalized dynamics of ball/cage and cage/race interactions is preserved. After discussing some general time scales in a ball bearing an overview of the computer program RAPIDREB will be presented below. The capabilties of RAPIDREB are demonstrated by simulating cage whirl in an engine bearing.

GENERAL TIME SCALES IN BALL BEARING DYNAMICS

The characteristic frequencies in the general dynamic performance of ball bearings normally cover a wide spectrum. Frequencies associated with the elastic contact phenomenon are on the high end while the shaft speed is on the low end of the spectrum. Fortunately for most operating environments the high frequencies are several orders of magnitude greater than the frequencies of the order of shaft revolution speed and therefore it is relatively easy to constrain the motion to eliminate all the high frequencies in order to look at the low frequency phenomenon in depth. To understand the physical mechanism behind each frequency the basic model for each interaction and the fundamental kinematics of ball motion must be reviewed.

Ball/Race Interaction

The normal contact loads at the ball/race interaction are computed by the Hertzian elastic contact theory. For small changes in load the non-linear Hertzian load-deflection relation can be suitably modeled as a linear spring. Now if the ball is free to translate arbitrarily a vibration frequency corresponding to this spring will be observed. This has been discussed in depth by Gupta et al (9). To review the phenomenon briefly Figure 1 shows typical axial and radial components of ball mass center as it travels in its orbit. Two distinct frequencies are seen in these acceleration patterns; the high frequency component corresponds to the elastic contact phenomenon, while the low frequency has a kinematic significance. For most ball bearings, depending on the bearing size, the elastic contact frequency is in the range of 1 to 50 kHz. The low frequency whose axial and radial components are 180 degrees out of phase, has been termed as a kinematic frequency (9) since it is a strong function of race curvatures and it is proportional to square root of ball/race contact load. Again the actual frequency for a given bearing depends on the geometry of the bearing and the applied conditions but the general range is from 500 Hz to 10 kHz.

Ball/Cage and Race/Cage Interactions

The dynamics of ball/cage interaction can be quite complicated depending on the operating conditions and the ball pocket clearances. For a simple thrust loaded condition with gravity acting along the bearing axis, the cage weight will be supported uniformly by all the balls and therefore ball/cage contact will be established in each pocket. Now, if the cage is free to translate axially, a vibratory motion of the cage relative to the balls, corresponding to the elastic spring which models the ball/cage contact, will be observed. Such a phenomenon is demonstrated in Figure 2. Again the frequencies will be generally high compared to the shaft rotational speed.

In most instances the ball/cage contacts may be of impulsive nature and the total time of contact may be very small. A typical example is presented in Figure 3. Such impulsive contacts will produce definite discontinuities in the motions of both the balls and the cage and considerable care will be required in integrating the equations of motion.

Low Frequency Components

This class of motion basically contains frequencies of the order of race angular velocities. The components of interest generally include ball angular velocity, ball orbital velocity, ball pass frequency (rate at which a given point on the race is passed by the balls), etc. All of these frequencies may not be constant depending on the operating conditions. In fact, the variation in ball angular velocity may sometimes be quite large. This can be easily illustrated if the equations of ball angular motion are written in a coordinate frame rotating with a velocity $\dot{\theta}$ which is also the ball orbital velocity:

$$I\dot{\omega}_1 = G_1$$

$$I\dot{\omega}_2 - I\omega_3\dot{\theta} = G_2$$

$$I\dot{\omega}_3 + I\omega_2\dot{\theta} = G_3$$

where I is the ball moment of inertia, $\vec{\omega}$ is the angular velocity and $\vec{G}$ is the applied moment vector.

If, for instance, the applied moment is zero, then ω_1 will be constant and ω_2 and ω_3 will be governed by

$$\dot{\omega}_2 - \omega_3\dot{\theta} = 0$$

$$\dot{\omega}_3 + \omega_2\dot{\theta} = 0$$

or

$$\ddot{\omega}_2 + \omega_2\dot{\theta}^2 = 0$$

$$\ddot{\omega}_3 + \omega_3\dot{\theta}^2 = 0$$

assuming $\dot{\theta}$ to be constant.

Thus both ω_2 and ω_3 will have a cyclic variation with a frequency of $\dot{\theta}$. The nature of the applied moment $\vec{G}$ and its dependence of ball angular velocity will of course greatly influence the ultimate motion of the balls.

For any given bearing application all of the above characteristic motions must be clearly understood before considering any constraints on the ball motion. In particular the knowledge of difference between the various components will be very useful and two classes of problems may be considered:

Class I: All frequencies are of the same general order

Class II: There is a distinct difference between the "very low" and "very high" frequency components.

Class I will be relevant for a relatively large bearing operating at very high speeds and Class II will apply to most small to moderate size bearings in a wide operating environment and large bearings operating at very low speeds. For the Class I system a generalized motion of each element must be determined as done by the author (4-7) in the original DREB program. However, for Class II applications certain constraints can be imposed and applications falling in this class are the subject of this paper.

OVERVIEW OF THE RAPIDREB CODE

The computer code RAPIDREB is an enhanced version of the original DREB program. The key enhancement consists of suppressing the very high frequencies in the performance simulation of ball bearings. Although similar modifications of DREB may be considered for roller bearings, RAPIDREB considers ball bearings only. If the race angular velocity is very small compared to the high frequency motion, a suppression of the high frequency components will not affect the components of the order of race angular velocity. Assuming that the vibratory motions being suppressed does indeed have frequencies much greater than the race angular velocities, two means of suppression may be considered, e.g., ball motion constraints and suitable damping.

Ball Motion Constraints

The very high frequency motion results from ball vibration between the two races. As discussed earlier, both the elastic contact frequency and the kinematic frequency represent the motion of ball mass center relative to the supporting races. If the applied load on the bearing is free of any high frequency vibrational component, the amplitudes of the ball vibration are generally small and the resulting changes in contact loads are fairly insignificant when compared with the nominal loads. It may therefore be reasonable to constrain the ball such that equilibrium of all normal contact forces acting on the ball including the centrifugal forces is satisfied at every instant of time. The traction forces, being quite small compared to the normal forces, may be neglected in the equilibrium equations. Such constraints are reasonable for all static applied loads and constant races speeds. They are also applicable to time varying loads and speeds provided the frequency of such variations is very small compared to the characteristic ball/race vibration frequencies. Thus moderate race accelerations and synchronous loading due to unbalance can be satisfactorily treated within the realm of such equilibrium constraints.

It is true that the process of imposing the above constraints is similar to obtaining the conventional quasi-static solutions at each time step and hence a set of non-linear algebraic equations has to be solved at each step. This may appear to be quite time consuming but even for relatively large steps, allowable by ball/race traction phenomenon, the changes in the equilibrium conditions are rather small and therefore the convergence of the equilibrium equations is very rapid. Thus a small increase in the computational effort per step substantially outweighs the permissible increase in step size as compared to the generalized case where all acceleration components are permitted.

Damping Considerations

There may be some damping considerations which can assist in eliminating certain high frequencies. It is true that actual damping at any contact interface in the bearing is quite small and therefore the introduction of any damping will be "fictitious" with the prime objective of eliminating the high frequency response without significantly altering the very low frequency behavior.

Any contact interface can be modeled in terms of a spring with stiffness k (N/M) and a dashpot with damping C (NS/M) as shown in Figure 4. The contact stiffness will be known from the Hertzian contact parameters at the particular contacts and the damping coefficient will be the required input. Perhaps specification of damping will be best in terms of a damping ratio C/C_c, where C_c is called critical damping (10) corresponding to the undamped natural frequency of the system.

Damping ratio $\zeta = C/C_c$

where $C_c = 2m\omega_n$

$$\omega_n = \sqrt{\frac{k}{m}}$$

Thus ζ can be specified for the ball/race, ball/cage and cage/race interfaces. For the purpose of "real" damping ζ will be very small for most steels but for certain nonmetals used for fabricating the cages it may be appreciable. In any event any non-zero value of ζ will only effect the general response in the neighborhood of the undamped natural frequency ω_n (10) and the response at very low frequencies will be practically unchanged.

RAPIDREB Outline

A schematic outline of the RAPIDREB code is presented in Figure 5. For a prescribed bearing and operating environment a conventional quasi-static analysis is first performed to compute the initial conditions for the integration of the differential equations of motion. With these initial conditions a real time simulation is then obtained by numerically integrating the equations of motion. All the generalized six-degrees-of-freedom are maintained except for those on the ball mass center, whose axial and radial positions are determined by the equilibrium constraint. Since this constraint is applied at each time step, dynamic variations in applied load are fully treated so long as such variations do not occur at very low frequencies of the order of those being suppressed by the constraint.

The option for fictitious damping is included in the input materials data, where arbitrary damping ratios can be prescribed for any interaction. RAPIDREB also offers the option of bypassing the equilibrium constraint and thereby reverting back to a form equivalent to the original DREB program. Thus generalized dynamic simulations may also be obtained to study the effect of damping and other dynamic factors in the high frequency range.

In addition to the above RAPIDREB contains the option of exercising a number of different integrating algorithms consisting of both explicit Runga-Kutta type formulae and the implicit predictor-corrector type schemes. Further details are described elsewhere (11).

TYPICAL RESULTS

RAPIDREB is executed for a number of different bearings and it is found that the reduction in computational effort by exercising the equilibrium constraint can range from a factor of 5 to 15 over the effort required by the DREB program. For very simple configurations, such as an angular contact ball bearing with pure thrust load, this factor may be as high as 100. However, it is found that the fictitious damping option does not provide any significant reduction in computational effort, a factor of two is perhaps a realistic upper limit.

In order to demonstrate the general capabilities of RAPIDREB performance simulations over several shaft revolutions are obtained for a high speed engine bearing. Details of the bearing and operating conditions are briefly discussed below before presenting the performance simulations.

Bearing Geometry

The geometry of the bearing is shown in the computer output in Appendix A. It is a 100 mm bore ball bearing with a steel cage guided on the inner race. The design corresponds to an actual test bearing.

Lubricant Traction Models

Conventional lubricant with the MIL-L-7808 specification is assumed. The traction behavior of this lubricant has been studied fairly extensively and the model in the original DREB program has been demonstrated to show a reasonable fit with the experimental data. The model is also built into RAPIDREB and appropriate input option is exercised to select the MIL-L-7808 model.

For the ball/cage and cage/race interfaces a hypothetical traction model (see Appendix A) is used to compute the friction forces when a metal contact takes place.

Operating Conditions

To simulate typical test conditions, the following operating conditions are assumed:

Axial load =	18,000 N
Radial load =	4,500 N
Inner race speed =	20,000 RPM
Outer race speed =	0
Operating temperature =	330°K

Gravity acts normal to the bearing axis. Radial and axial equilibrium constraints on ball motion are assumed to eliminate the high frequency ball/race vibrations. Also the quasi-static solutions are used to determine the initial conditions.

Performance Simulations

Performance simulations for the engine bearing at the above conditions are obtained over seven shaft revolutions and hence definite steady state behavior can be easily understood. Typical initial parameters are illustrated in the computer output presented in Appendix A. Results presented below are in terms of computer plots of dimensionless variables as provided by RAPIDREB. Appropriate dimensional values may be obtained by using the scale factor contained in the computer output in Appendix A.

As might be expected in case of combined axial and radial load, the ball load and contact angles go through a cyclic variation with a frequency corresponding to the ball orbital velocity. This is seen in Figure 6 where over three wavelengths of variations corresponding to over seven shaft revolutions are shown. Also the spin/roll ratios in Figure 6 show that the race-control hypothesis does not hold and definite relative spin velocities develop in steady-state. Ball angular velocities demonstrate an interesting effect, see Figure 7. Since the initial quasi-static solutions do not allow for the gyroscopic slip and the exact equilibrium of gyroscopic moments, the ball immediately tends to slip about the transverse y axis due to gyroscopic moments. This alters the x and z components also and it takes approximately two shaft revolutions for the angular velocities to develop some steady state pattern and satisfy the gyroscopic slip as permitted by the lubricant characteristics. The ball/cage interactions show that about one collision in each pocket takes place per revolutions of the cage and the ball drives the cage (ball/cage contact angle of 180 degrees) for part of the revolution and gets driven by the cage (contact angle of zero) for the remaining part. This is seen in Figure 8. The ball/cage forces seen in this figure are really the collision forces and the hydrodynamic forces, being quite small compared to the collision forces, are not seen in the figure. However, the ball/cage approach relative to the radial pocket clearance clearly demonstrates the transition from hydrodynamic to metal contact.

The race/cage interaction is very dynamic and interesting to note. Figure 9 shows the race/cage force variations at the two lands (labeled 1 and 2) on either side of the balls. Initially the collision forces on both lands are identical but when appreciable coning motion of the cage develops, the forces on the two lands begin to differ; this is more clear from the traction force curves. The ultimate behavior to note is that the race/cage collisions are really very close together in time in steady state. Also the magnitude of the force is fairly large ($\sim$1800 N). This means that the cage will steadily be in contact with the race with a relatively large force, and some cage wear problems may be expected. This is seen by the steady circular orbit of the cage mass center in Figure 10 with the orbit radius equal to the cage/race radial clearance. This effect has indeed been confirmed experimentally (12) and the experimental results will soon be documented elsewhere (13).

Corresponding to the above race/cage collisions considerable radial chatter of the cage mass is observed, as shown in Figure 11 in terms of the cage mass center velocities. Excessive whirl is indicated by the increased orbital velocity. The coning motion is demonstrated by the angular velocity variations in Figure 12. The deviation of cage angular velocity from the initial epicyclic angular velocity (see component x) indicates substantial skid in the bearings due to excessive rubbing of the cage at the cage/race interface. The cage whirl and skid are sometimes better understood in terms of the cage orbital to angular and cage angular to shaft angular velocity ratios plotted in Figure 13.

Finally, the variations of bearing torque, power loss, and the cumulative load slip integral are shown in Figure 14. The initial bump in the torque curves correspond to the gyroscopic slip of the balls as discussed above and the steady noise is a result of the ball/cage and race/cage collisions.

SUMMARY

The existing Dynamics of Rolling Element Bearings (DREB) computer program has been enhanced to selectively suppress the very high frequency vibratory motion of the balls in an angular contact ball bearing and thereby provide the added capability of investigating the low frequency phenomena in some depth. With such an enhancement a considerable increase in the maximum permissible time step size has led to bearing performance simulation over several shaft revolutions within reasonable computing effort.

In order to demonstrate the capabilities of RAPIDREB, performance simulations are obtained for a typical high speed engine bearing with a combined thrust and radial load (thrust to radial load ratio of 4) over more than seven shaft revolutions. The test example consists of a 100 mm bore ball bearing operating at 20,000 rpm with a thrust load of 18000 N and a radial load of 4500 N. The bearing uses a steel cage guided on the inner race. It is shown that for such an operating environment the cage develops appreciable whirl velocity and in steady state a continued metal contact at the guiding land is established. Hence a definite possibility of cage wear at the guiding surface is simulated.

ACKNOWLEDGEMENTS

This work has been sponsored by the U. S. Air Force Materials Laboratory, Wright-Patterson Air Force Base, Ohio under contract number F33615-80-C-5152. The Air Force project manager was Dr. Howard Bandow at the Materials Laboratory. Computer facilities were provided by the ASD Computer Center at Wright-Patterson Air Force Base, Ohio and the Courant Institute of Mathematical Sciences at the New York University, New York, New York.

REFERENCES

1. Gupta, P.K., "A Review of Computerized Simulation of Roller Bearing Performance," ASME Publication "Computer-Aided Design of Bearings and Seals" edited by F.E. Kennedy and H.S. Cheng, Proc. of Winter Annual Meeting, Dec. 5-10, 1976, pp. 19-30.

2. Sibley, L.B. and Pirvics, J., "Computer Analysis of Rolling Bearings", ASME Publication "Computer-Aided Design of Bearings and Seals" edited by F.E. Kennedy and H.S. Cheng, Proc. of Winter Annual Meeting, Dec. 5-10, 1976, pp. 95-115.

3. Walters, C.T., "The Dynamics of Ball Bearings," J. Lub. Tech., ASME Trans., Series F, Vol. 93, 1971, pp. 17-24.

4. Gupta, P.K., "Dynamics of Rolling Element Bearings - Part I: Cylindrical Roller Bearing Analysis," Trans. ASME, J. Lub. Tech., Vol. 101, No. 3, July 1979, pp. 293-304.

5. Gupta, P.K., "Dynamics of Rolling Element Bearings - Part II: Cylindrical Roller Bearing Results," Trans. ASME, J. Lub. Tech., Vol. 101, No. 3, July 1979, pp. 305-311.

6. Gupta, P.K., Dynamics of Rolling Element Bearings - Part III: Ball Bearing Analysis," Trans. ASME, J. Lub. Tech., Vol. 101, No. 3, July 1979, pp. 312-318.

7. Gupta, P.K., "Dynamics of Rolling Element Bearings - Part IV: Ball Bearing Results," Trans. ASME, J. Lub. Tech., Vol. 101, No. 3, July 1979, pp. 319-326.

8. Brown, P.F., et al. "Development of Mainshaft High-Speed Cylindrical Roller Bearings for Gas Turbine Engines", Technical Report #NAPC-PE-60C, prepared for Naval Air Propulsion Center, Trenton, N.J., Contract N00140-76-C-0383, Nov. 1980.

9. Gupta, P.K., Winn, L.W., and Wilcock, D.F., "Vibrational Characteristics of Ball Bearings, J. Lub. Tech., ASME Trans., 99F, #2, pp. 284-289, (1977).

10. Den Hartog, J.P., Mechanical Vibrations, McGraw Hill Book Company, 1956.

11. Gupta, P.K., "Interactive Graphic Simulation of Rolling Element Bearings, Phase I: Low Frequency Phenomenon and RAPIDREB Development," U. S. Air Force Technical Report AFWAL-TR-81-4148, Contract number F33615-80-C-5152, November 1981.

12. Dill, J.F., Personal Communications.

13. Dill, J.F. and Gupta, P.K., "Experimental Validation of the DREB Computer Program in the Engine Bearing Operating Environment," to be published.

APPENDIX A

TYPICAL COMPUTER OUTPUT FOR THE 100 mm ENGINE BEARING

```
RRRRRRRRRRRRRRR     DDDDDDDDDDDDDDD     PRRRRRRRRRRRRRR     EEEEEEEEEEEEEEEE     BBBBBBBBBBBBBBBB
RRRRRRRRRRRRRRRR    DDDDDDDDDDDDDDDD    RRRRRRRRRRRRRRRR    EEEEEEEEEEEEEEEE    BBBBBBBBBBBBBBBBB
  RR          RR      DD          DD      RR          RR      EE                    BB          BB
  RR          RR      DD          DD      RR          RR      EE                    BB          BB
  RRRRRRRRRRRRR       DD          DD      RRRRRRRRRRRRR       EEEEEEEEEE            BBBBBBBBBBBB
  RRRRRRRRRRRR        DD          DD      RRRRRRRRRRRR        EEEEEEEEEE            BBBBBBBBBBBB
  RR        RR        DD          DD      RR        RR        EE                    BB          BB
  RR         RR       DD          DD      RR         RR       EE                    BB          BB
  RR          RR      DD          DD      RR          RR      EE                    BB          BB
  RR           RR     DDDDDDDDDDDDDDD     RR           RR     EEEEEEEEEEEEEEEE      BBBBBBBBBBBBBBB
  RR           RR     DDDDDDDDDDDDDD      RR           RR     EEEEEEEEEEEEEEEE      BBBBBBBBBBBBBBB

                    R A P I D     S I M U L A T I O N     O F     T H E

    D Y N A M I C S     O F     R O L L I N G     E L E M E N T     B E A R I N G S

                        -A REAL TIME PERFORMANCE SIMULATION-
                              (VERSION RAPIDREB,01)

                                  PRADEEP K. GUPTA
                            MECHANICAL TECHNOLOGY INCORPORATED
                                968 ALBANY-SHAKER ROAD
                                  LATHAM, NEW YORK
                                     U. S. A.
```

BEARING TYPE -- BALL SPEC CODE -- 100MM ENGINE BRG MOD CAGE 18/4.5KN 20KRPM

BEARING GEOMETRY

BORE	(M)	= 1.00000E-01	OUTER RACE SHRINK FIT	(M)	=	1.00000E-05
OUTSIDE DIAMETER	(M)	= 1.80000E-01	INNER RACE SHRINK FIT	(M)	=	5.00000E-05
SHAFT INNER DIA	(M)	= 2.00000E-02	HOUSING OUTER DIA	(M)	=	2.05000E-02
BALL DIAMETER	(M)	= 1.905000E-02	NUMBER OF BALLS		=	18
PITCH DIAMETER	(M)	= 1.40000E-01	OUTER RACE CUR FACTOR		=	5.20000E-01
CONTACT ANGLE	(DEG)	= 2.50000E+01	INNER RACE CUR FACTOR		=	5.40000E-01
END PLAY	(M)	= 9.66105E-04	DIAMETRAL PLAY	(M)	=	2.14180E-04

```
        CAGE OUTER DIA      (M) =  1.48800E-01       CAGE OUTER DIA CLS       (M) =  7.00000E-03
        CAGE INNER DIA      (M) =  1.29700E-01       CAGE INNER DIA CLS       (M) =  3.00000E-03
        EFF CAGE WIDTH      (M) =  2.73000E-02       DIA RE/CAGE CLEARANCE    (M) =  8.26000E-04

                    GUIDANCE    GUIDING RACE         GUIDING CAGE       EFF  LAND       CAGE  HALF
                        TYPE    RADIUS   (M)         RADIUS   (M)       WIDTH  (M)      WIDTH  (M)

        GUIDING LAND  I     2      6.42350E-02          6.48500E-02     4.00000E-03     1.36500E-02
        GUIDING LAND II     2      6.42350E-02          6.48500E-02     4.00000E-03     1.36500E-02


LUBRICATION DETAILS
-------------------

 1. ROLLING ELEMENT/CAGE AND RACE/CAGE PARAMETERS ---

                                                 INTERACTION  LUB VISCOSITY        MAX FILM
                                                        CODE     (N*S/M**2)           (M)

    ROLLING ELEMENT/CAGE INTERACTION                       1     7.12466E-03    4.00000E-04
    RACE/CAGE INTERACTION                                  1     7.12466E-03


    RE/CAGE DRY CONTACT TRACTION PARAMETERS --

    CRIT FILM THICKNESS  (M)      =  5.00000E-07
    TRAC COEFF AT ZERO SLIP       =  0.                 MAXIMUM TRAC COEFF              =  2.00000E-02
    TRAC COEFF AT INFINITE SLIP   =  1.60000E-02        SLIP AT MAX TRAC       (M/S)    =  1.00000E+00


    CAGE/RACE DRY CONTACT TRACTION PARAMETERS --

    CRIT FILM THICKNESS  (M)      =  5.00000E-07
    TRAC COEFF AT ZERO SLIP       =  0.                 MAXIMUM TRAC COEFF              =  2.00000E-02
    TRAC COEFF AT INFINITE SLIP   =  1.60000E-02        SLIP AT MAX TRAC       (M/S)    =  1.00000E+00

 2. ROLLING ELEMENT/RACE PARAMETERS (TRACTION CODE = 3) ---

    FILM THICKNESS CODE            =             2      CRIT FILM THICKNESS    (M)      =  1.00000E-07
    INLET TEMP           (DEG-K)   =  3.30000E+02       PR-VIS COEFF           (M**2/N) =  1.01447E-08
    INLET VIS         (N*S/M**2)   =  7.12466E-03       TEMP-VIS COEFF         (DEG-K)  =  2.85205E+03
    THERMAL COND      (N/S/DEG-C)  =  9.65788E-02       STARVATION PARAMETER            =  1.00000E+01

    VISCOCITY*        (N*S/M**2)   =  7.87989E-02       ROLLING SPEED EFFECT
    PR-VIS COEFF*       (M**2/N)   =  5.22136E-09       PARAMETERS -  VR       (M/S)    =  2.28600E+01
    TEMP-VIS COEFF*    (1/DEG-K)   =  5.46451E-02                     VN                = -7.03200E-01

    OUTER RACE TEMP      (DEG-K)   =  3.30000E+02       INNER RACE TEMP        (DEG-K)  =  3.30000E+02

 3. TRACTION PARAMETERS OUT OF LUB MODEL BOUNDS ---

    TRAC COEFF AT ZERO SLIP       =  0.                 MAXIMUM TRAC COEFF              =  2.00000E-02
    TRAC COEFF AT INFINITE SLIP   =  1.60000E-02        SLIP AT MAX TRAC       (M/S)    =  1.00000E+00

 4. LUBRICANT DRAG AND CHURNING PARAMETERS ---

    EFF LUB VIS       (N*S/M**2)   =  7.12466E-03       EFF LUB DEN       (KGM/M**3)    =  1.00000E+01


APPLIED LOADS AND SPEEDS
------------------------

 1. QUASI-STATIC SIMULATION ---

    AXIAL  LOAD               (N)  =  1.80000E+04       OUTER RACE ANG VEL  (RPM)  =  0.
    RADIAL LOAD               (N)  =  4.50000E+03       INNER RACE ANG VEL  (RPM)  =  2.00000E+04
    RELATIVE MISALIGNMENT  (DEG)   =  0.

 2. DYNAMIC SIMULATION ---

                   *************** LOADS    (N) ************       ******** MASS CEN ACC   (M/S**2) ********
                           I               II              III                 I               II              III

    OUTER RACE                                                         0.              0.              0.
    INNER RACE                                                         0.              0.              0.

                   ************ MOMENTS    (N*M) ***********       ******** ANG ACCELERATION (RPM/S) *******
                           I               II              III                 I               II              III

    OUTER RACE                                                         0.              0.              0.
    INNER RACE                                                         0.              0.              0.

                   ******** ANGULAR VELOCITIES (RPM)********
                           I               II              III

    OUTER RACE     0.              0.              0.
    INNER RACE     2.00000E+04     0.              0.

    COMPONENTS OF ACCELERATION DUE TO GRAVITY VECTOR      (M/S**2) =  0.              0.              9.81000E+00

    EXTERNALLY APPLIED FORCE VECTOR ACTING ON CAGE              (N) =  0.              0.              0.
    CORRESPONDING POSITION VECTOR IN INERTIAL FRAME             (M) =  1.36500E-02     0.              0.
```

MATERIAL PROPERTIES AND INERTIAL PARAMETERS

		ROLLING ELEMENT	CAGE	RACEWAYS	SHAFT	HOUSING
ELASTIC MODULUS	(N/M**2)	1.99948E+11	2.00000E+11	1.99948E+11	1.99948E+11	1.99948E+11
POISSON-S RATIO		2.50000E-01	2.50000E-01	2.50000E-01	2.50000E-01	2.50000E-01
MASS DENSITY	(KGM/M**3)	7.75037E+03	7.75037E+03	7.75037E+03	7.75037E+03	7.75037E+03

		ROLLING ELEMENT	CAGE	OUTER RACE	INNER RACE
MASS	(KGM)	2.80547E-02	4.70585E-01	2.32900E+00	1.62894E+00
MOM OF INER -X	(KGM*M**2)	1.01811E-06	2.29196E-03	1.59413E-02	5.50250E-03
MOM OF INER -Y	(KGM*M**2)	1.01811E-06	1.17521E-03	8.25241E-03	2.94830E-03
MOM OF INER -Z	(KGM*M**2)	1.01811E-06	1.17521E-03	8.25241E-03	2.94830E-03

BALL/RACE DAMPING RATIO = 0.
BALL/CAGE DAMPING RATIO = 0.
RACE/CAGE DAMPING RATIO = 0.

SCALE FACTORS, INTEGRATION DETAILS AND OUTPUT CONTROLS

LENGTH SCALE (M) = 9.52500E-03 MIN STEP SIZE = 2.00000E-02 INITIAL STEP SIZE = 1.00000E-01
LOAD SCALE (N) = 1.80000E+04 MAX STEP SIZE = 1.00000E+01 TRUNCATION LIMIT = 1.00000E-04
TIME SCALE (S) = 1.21843E-04 FINAL TIME = 4.00000E+02 STEP OPT CODES = 6 50 2

DATA MONITOR CODE =200 PRINT CODES = 5 50 5 AUTO PLOT CODES = 1 19 21
INT METHOD CODE = 0 SOLUTION MODE = 3

OUTPUT FROM USER ACCESSIBLE ROUTINES ---

STEP NO 1 TAU = 0. TIME = 0. S 100MM ENGINE BRG MOD CAGE 18/4.5KN 20KRPM

ROLLING ELEMENT PARAMETERS

RE NO	CONTACT ANGLES (DEG) OUTER RACE	OUTER RACE	INNER RACE	INNER RACE	CONTACT LOADS (N) OUTER RACE	INNER RACE	CONTACT DEFLS (M) OUTER RACE	INNER RACE	CONTACT STRESSES (N/M**2) OUTER RACE	INNER RACE
1	1.599E+01	0.	2.527E+01	0.	4.420E+03	2.852E+03	2.350E-05	2.098E-05	1.921E+09	2.147E+09
7	1.434E+01	0.	2.640E+01	-4.467E-03	3.599E+03	2.005E+03	2.049E-05	1.658E-05	1.793E+09	1.908E+09
13	1.434E+01	0.	2.640E+01	4.467E-03	3.599E+03	2.005E+03	2.049E-05	1.658E-05	1.793E+09	1.908E+09

RE NO	CONTACT HALF WIDTHS (M) OUTER RACE	INNER RACE	OUTER RACE	INNER RACE	LOAD*SLIP INTEGRALS (N*M/S) OUTER RACE	INNER RACE	TRAC*SLIP INTEGRALS (N*M/S) OUTER RACE	INNER RACE	SPIN/ROLL RATIOS OUTER RACE	INNER RACE
1	2.880E-03	1.934E-03	3.815E-04	3.281E-04	2.099E+03	4.124F+03	3.039E+01	7.434E+01	-3.606E-15	2.311E-01
7	2.689E-03	1.719E-03	3.564E-04	2.919E-04	1.496E+03	3.055F+03	1.692E+01	5.088E+01	6.642E-16	2.754E-01
13	2.689E-03	1.719E-03	3.564E-04	2.919E-04	1.496E+03	3.055E+03	1.692E+01	5.088E+01	1.727E-15	2.754E-01

RE NO	ORB POS (DEG)	MASS CENTER VELOCITIES (M/S) AXIAL	(M/S) RADIAL	(RPM) ORBITAL	ANGULAR VELOCITIES (RPM) X COMP	Y COMP	Z COMP	RE/CAGE CON FORCES (N) NORMAL	(N) TRACTION	(DEG) CON ANGLE
1	0.	0.	0.	8.804E+03	-7.143E+04	0.	1.794E+04	2.149E-02	2.617E-02	2.700E+02
7	1.200E+02	0.	0.	8.859E+03	-7.232E+04	0.	1.622E+04	1.276E+00	2.217E-01	1.791E+02
13	2.400E+02	0.	0.	8.859E+03	-7.232E+04	0.	1.622E+04	1.276E+00	2.217E-01	8.611E-01

RE NO	RE/CAGE MIN CLS (M)	RE/CAGE SLIP VELS (M/S)	RE/RACE SLIP VELOCITIES (M/S) OUTER RACE I	OUTER RACE II	INNER RACE I	INNER RACE II	RE/RACE TRACTION COEFFICIENTS OUTER RACE I	OUTER RACE II	INNER RACE I	INNER RACE II
1	4.050E-04	1.790E+01	0.	-3.523E-01	0.	0.	0.	-2.000E-02	0.	0.
7	1.471E-04	7.392E+01	0.	-3.087E-01	-1.407E-03	-5.555F-13	0.	-2.000E-02	-1.405E-13	-1.405E-13
13	1.471E-04	7.392E+01	-3.439E-14	-3.087E-01	1.407E-03	0.	-2.228E-15	-2.000E-02	0.	0.

RE NO	RE/RACE ISO FILM (M) OUTER RACE	INNER RACE	THERMAL*SIDE LEAKAGE FACTORS OUTER RACE	INNER RACE	DRAG FORCE (N)	CHURN MOM (N*M)	NET DRAG+ CHURN LOSS (N*M/S)
1	1.043E-06	9.395E-07	3.798E-01	3.783E-01	2.731E+00	2.880E-03	1.986E+02
7	1.063E-06	9.597E-07	3.818E-01	3.886E-01	2.766E+00	2.907E-03	2.023E+02
13	1.063E-06	9.597E-07	3.818E-01	3.886E-01	2.766E+00	2.907E-03	2.023E+02

STEP NO 1 TAU = 0. TIME = 0. S 100MM ENGINE BRG MOD CAGE 18/4.5KN 20KRPM

RACE AND CAGE PARAMETERS

	**** MASS CENTER POSITIONS **** (M) AXIAL	(M) RADIAL	(DEG) ORBITAL	**** MASS CENTER VELOCITIES **** (M/S) AXIAL	(M/S) RADIAL	(RPM) ORBITAL	***** ANGULAR POSITIONS ******* (DEG) X COMP	Y COMP	Z COMP
CAGE	-5.760E-05	3.070E-04	0.	0.	0.	0.	0.	0.	0.
OUTER RACE	0.	0.	0.	0.	0.	0.	0.	0.	0.
INNER RACE	-3.747E-05	7.039E-06	0.	0.	0.	0.	0.	0.	0.

	****** ANGULAR VELOCITIES ****** (RPM) X COMP	Y COMP	Z COMP	******** NET ACC FORCES ******** (N) X COMP	Y COMP	Z COMP	******** NET ACC MOMENTS ******* (N*M) X COMP	Y COMP	Z COMP
CAGE	8.841E+03	0.	0.	3.288E-03	-2.478E+00	-9.451E+00	1.161E-01	2.544E-02	2.983E-02
OUTER RACE	0.	0.	0.	1.800E+04	-1.932E+01	4.364E+03	-1.462E+01	1.312E+02	-2.829E-02
INNER RACE	2.000E+04	0.	0.	-1.800E+04	-3.820E+00	-4.498E+03	3.108E-01	-1.332E+02	-1.170E-01

	************ RACE/CAGE FORCES ************ (N) NORMAL	(N) TRACTION	(DEG) CON ANGLE	(DEG) ATT ANGLE	RACE/CAGE MIN CLS (M)	RACE/CAGE SLIP VELS (M/S)	EFFECTIVE DIA PLAY (M)
LAND NO 1	8.395E-02	1.753E+00	1.800E+02	-5.230E+01	2.781E-04	7.459E+01	1.156E-03
LAND NO 2	8.395E-02	1.753E+00	1.800E+02	-5.230E+01	2.781E-04	7.459E+01	1.156E-03

CAGE CHURN MOM (N*M) = 7.962E-02 CAGE NET CHURN LOSS (N*M/S) = 6.153E+02

APPLIED PARAMETERS

	************ FORCES ************ (N) X COMP	Y COMP	Z COMP	************ MOMENTS ********** (N*M) X COMP	Y COMP	Z COMP
OUTER RACE	-1.800E+04	1.932E+01	-4.364E+03	1.462E+01	-1.312E+02	2.829E-02
INNER RACE	1.800E+04	3.820E+00	4.498E+03	-3.108E-01	1.332E+02	1.170E-01

	** MASS CENTER ACCELERATIONS *** (M/S**2) X COMP	Y COMP	Z COMP	**** ANGULAR ACCELERATIONS **** (RPM/S) X COMP	Y COMP	Z COMP
OUTER RACE	0.	0.	0.	0.	0.	0.
INNER RACE	0.	0.	0.	0.	0.	0.

NET BRG LOSS (N*M/S) = 6.182E+03
CURRENT LIFE (HOURS) = 1.536E+03
INTERNAL CLEARANCE (M) = 1.062E-04
O.R. HOOP (N/M**2) = -1.427E+07
CAGE HOOP (N/M**2) = 3.511E+07

NET LOAD*SLIP (N*M/S) = 9.324E+04
OUTER RACE FIT (M) = 1.000E-05
INNER RACE FIT (M) = 9.767E-07
I.R. HOOP (N/M**2) = 1.183E+08

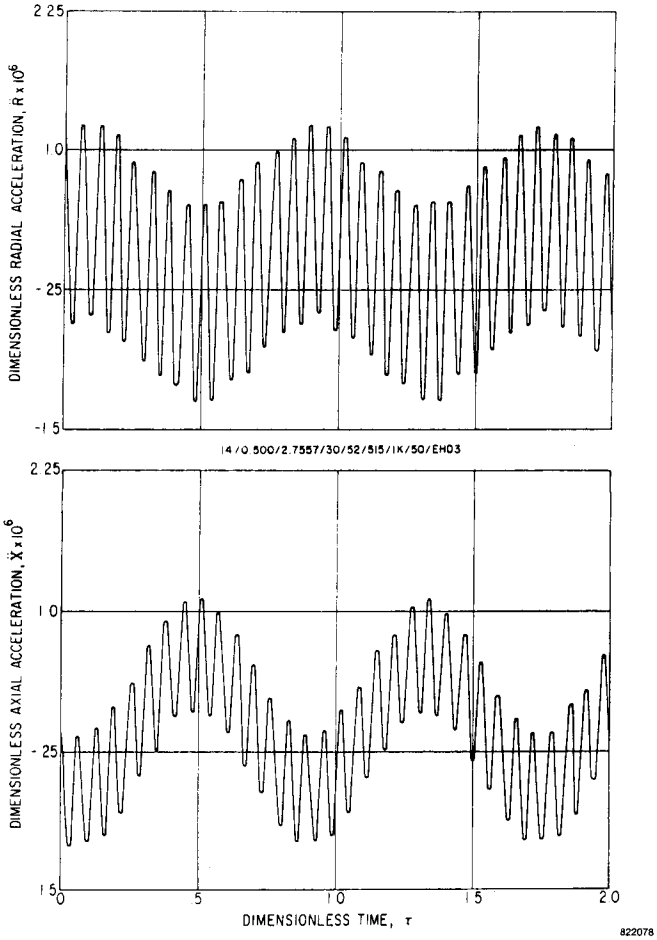

Fig. 1 Characteristic Ball Mass Center Vibration Pattern in an Angular Contact Ball Bearing

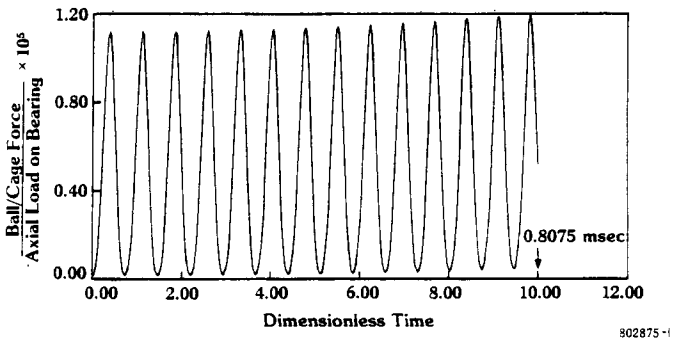

Fig. 2 Typical Ball/Cage Contact Vibration

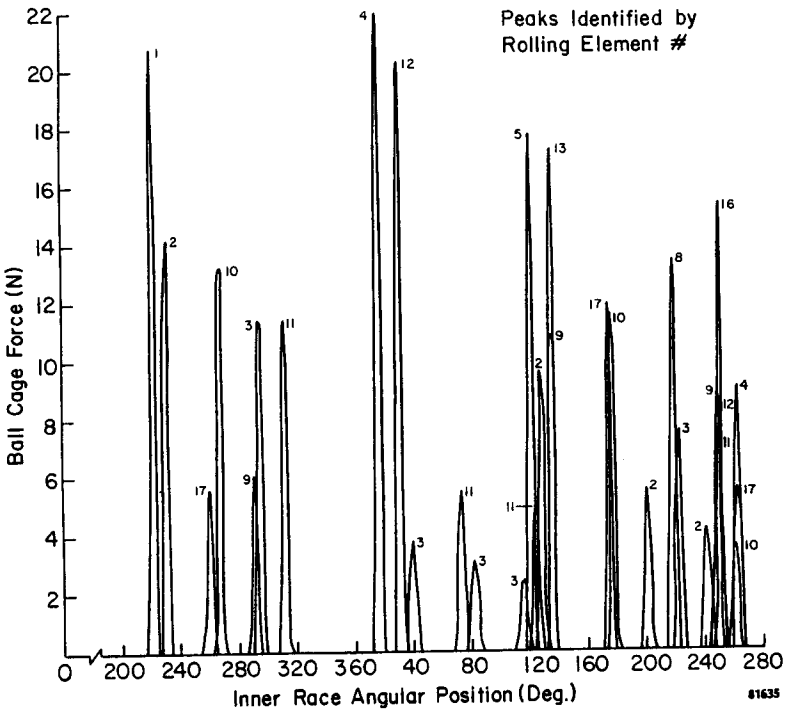

Fig. 3 Typical Ball/Cage Collisions in a Angular Contact Ball Bearing with Combined Axial and Radial Load

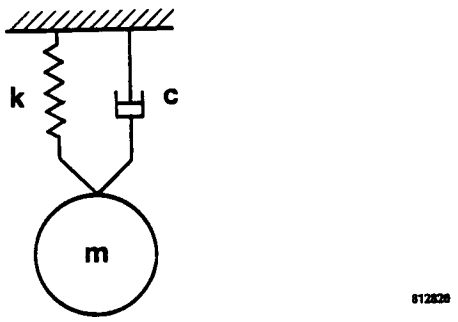

Fig. 4 Simple Spring and Damper Model for any Contact Interface

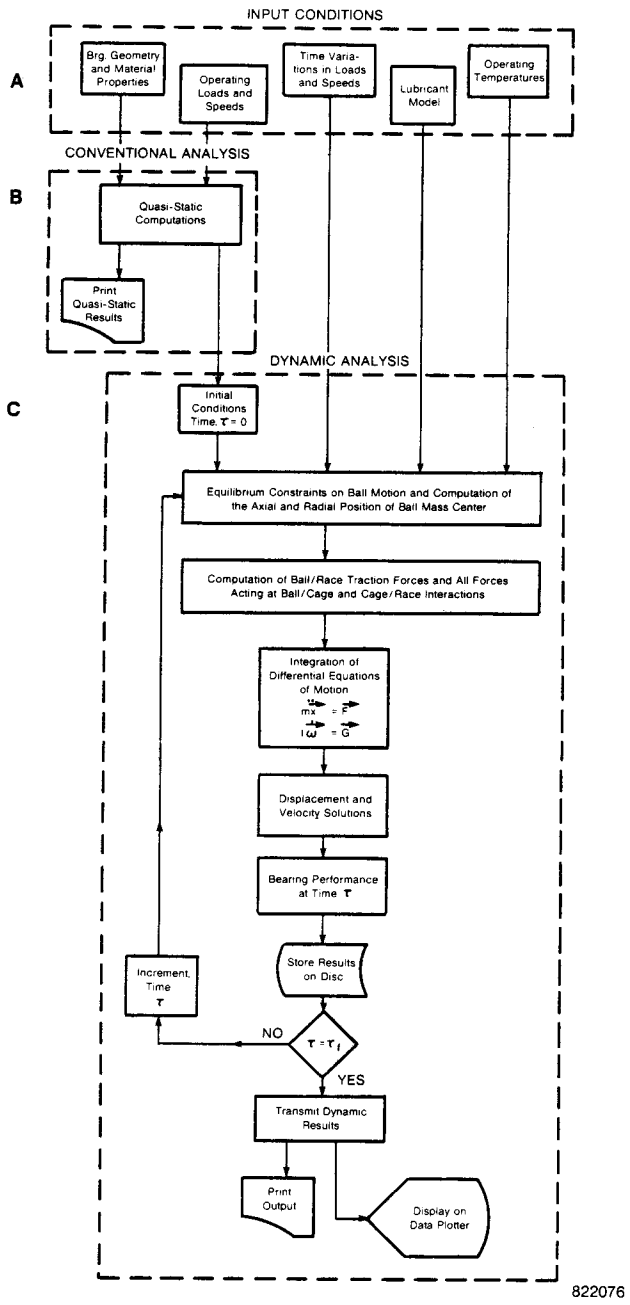

Fig. 5 A Schematic Overview of the RAPIDREB Computer Program

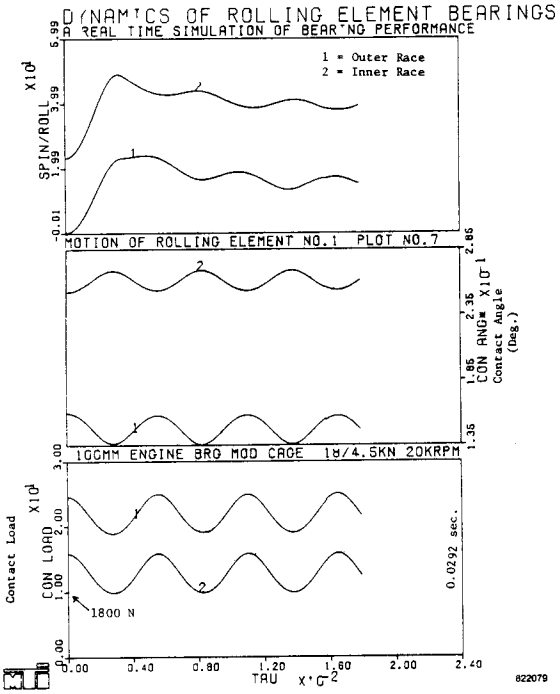

Fig. 6 Variations in Ball/Race Load, Contact Angle and Spin-to-Roll for the 100 mm Engine Bearing

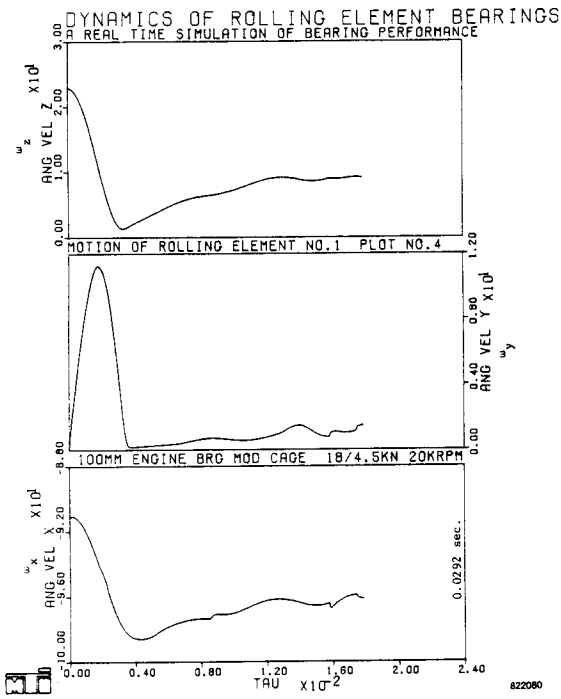

Fig. 7 Dimensionless Ball Angular Velocity Variation for the 100 mm Engine Bearing. Scale = 7.84×10^4 rpm

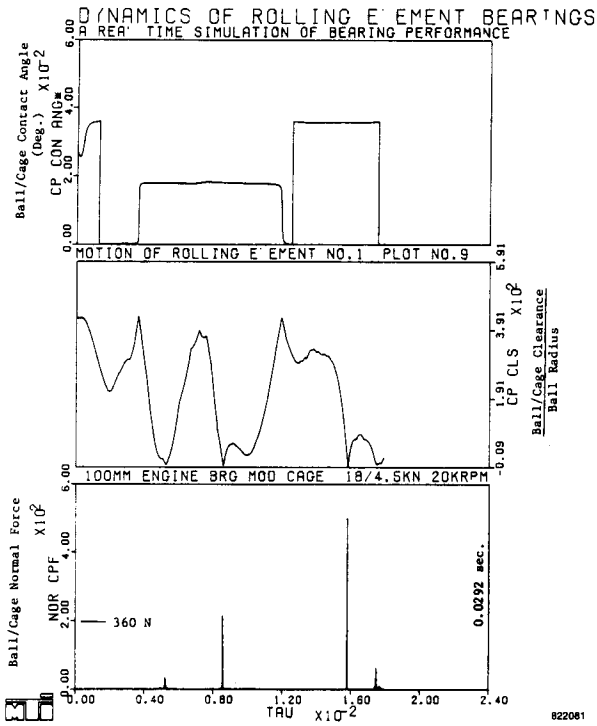

Fig. 8 Ball/Cage Interaction for the 100 mm Engine Bearing

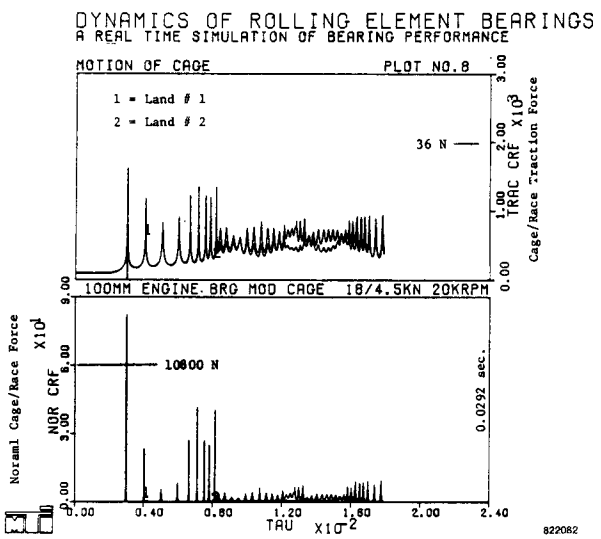

Fig. 9 Repeated Cage/Race Collisions in the 100 mm Engine Bearing

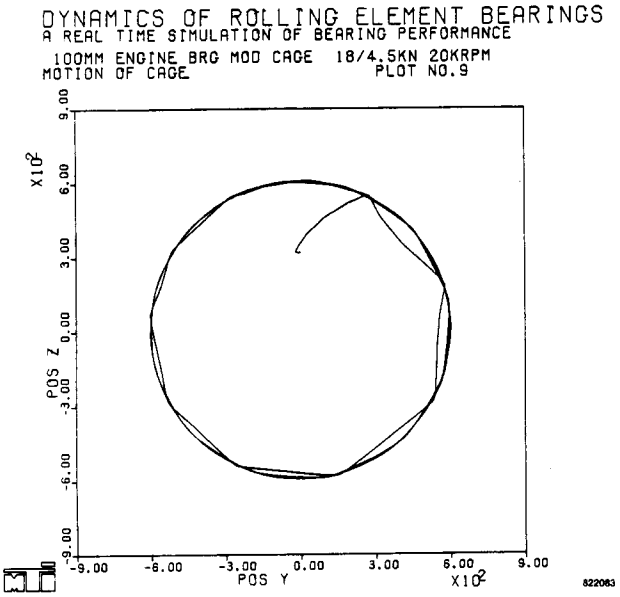

Fig. 10 Steady Orbit of the Cage Mass Center for the 100 mm Engine Bearing. Scale = 0.009525 M

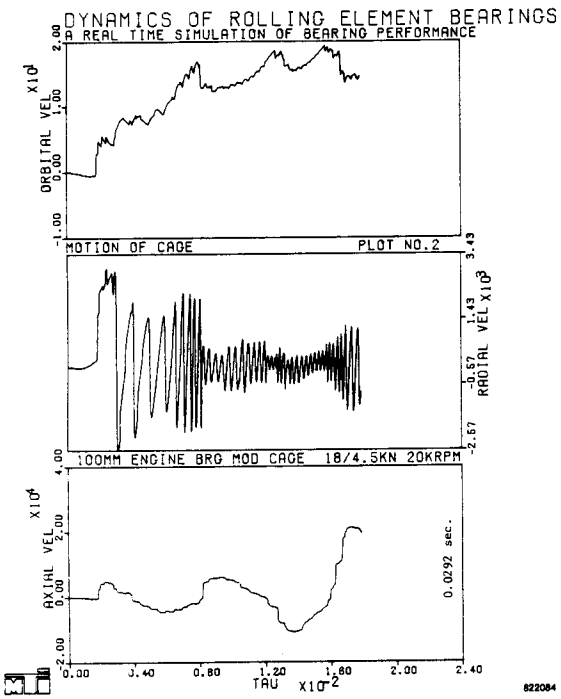

Fig. 11 Dimensionless Velocity of Cage Mass Center for the 100 mm Engine Bearing. Scales = 78.17 M/Sec., 7.84 x 10^4 rpm

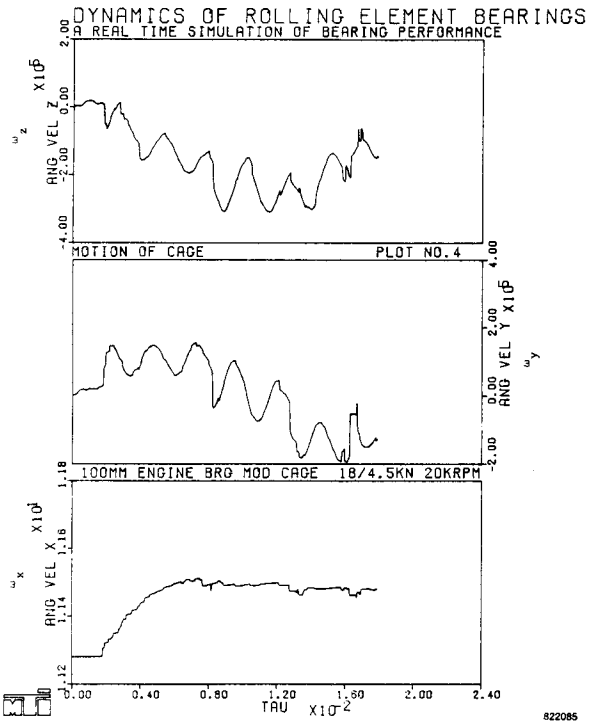

Fig. 12 Dimensionless Angular Velocity of a Ball in the 100 mm Engine Bearing. Scale = 7.84 x 10^4 rpm

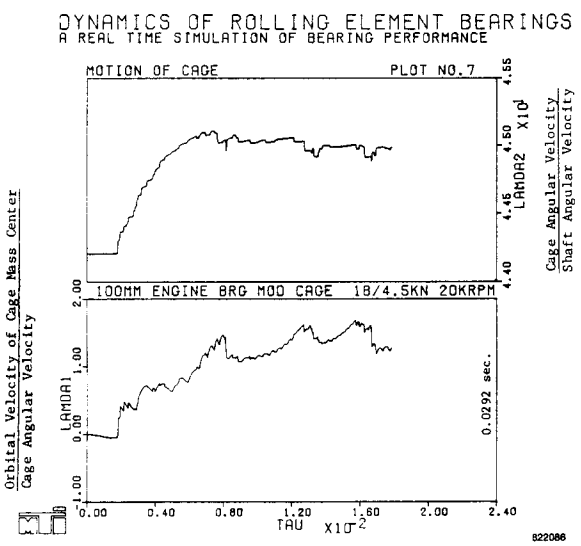

Fig. 13 Cage Whirl and Skid Parameters for the 100 mm Engine Bearing

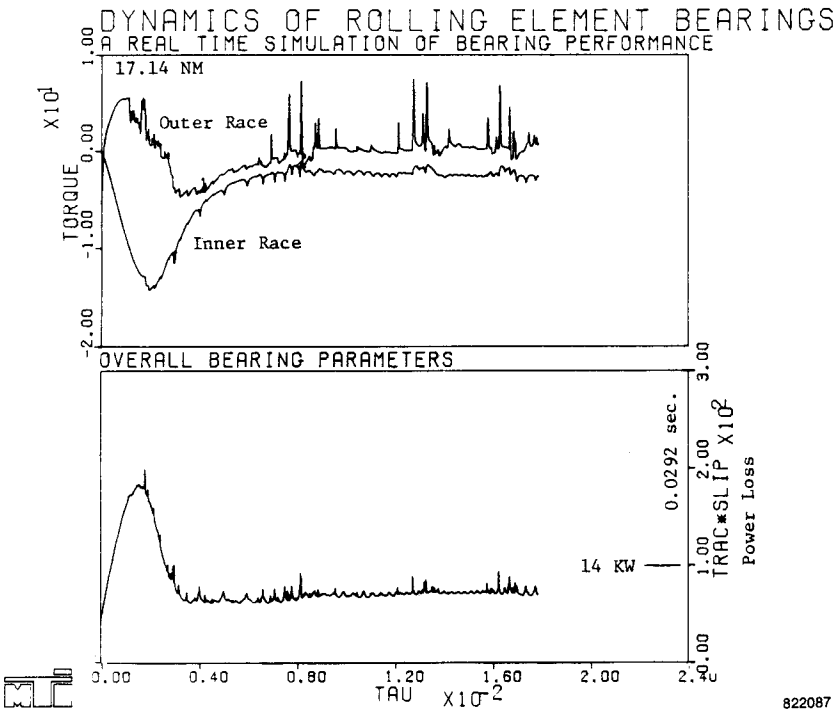

Fig. 14 Bearing Torque and Power Loss Variations in the 100 mm Engine Bearing